Images of a Spin-Torque-Driven Magnetic Nano-Oscillator

X. W. Yu, V. S. Pribiag, Y. Acremann, A. A. Tulapurkar, T. Tyliszczak, K. W. Chou, B. Bräuer, Z.-P. Li, O. J. Lee, P. G. Gowtham, D. C. Ralph, R. A. Buhrman, and J. Stöhr

Phys. Rev. Lett. **106**, 167202 — Published 21 April 2011

DOI: 10.1103/PhysRevLett.106.167202

Images of a Spin-Torque Driven Magnetic Nano-Oscillator

X. W. Yu,[1,*] V. S. Pribiag,[2,*] Y. Acremann,[3] A. A. Tulapurkar,[3] T. Tyliszczak,[4] K. W. Chou,[4] B. Bräuer,[3] Z.-P. Li,[2] O. J. Lee,[2] P. G. Gowtham,[2] D. C. Ralph,[2] R. A. Buhrman,[2] and J. Stöhr[3]

[1]*Department of Applied Physics, Stanford University, Stanford, California 94305, USA*
[2]*Cornell University, Ithaca, NY 14853, USA*
[3]*SLAC National Accelerator Laboratory, Menlo Park, California, 94025, USA*
[4]*Advanced Light Source, Berkeley, California 94720, USA*

We present the first space- and time-resolved images of the spin-torque-induced steady-state oscillation of a magnetic vortex in a spin valve nanostructure. We find that the vortex structure in a nanopillar is considerably more complicated than the 2D idealized structure often assumed, which has important implications for the driving efficiency. The sense of the vortex gyration is uniquely determined by the vortex core polarity, confirming that the spin torque acts as a source of negative damping even in such a strongly-nonuniform magnetic system. The orbit radius is ∼10 nm, in agreement with micromagnetic simulations.

PACS numbers: 85.75.-d, 72.25.-j, 75.75.Jn, 72.25.Pn

It has been suggested [1, 2] and verified [3–5] that spin torque can lead to steady-state precession of magnetization, forming the basis for highly-tunable microwave nano-oscillators. Research on spin-torque-induced microwave emission has until recently largely focused on magnetic systems with strong anisotropies and single-domain-like configurations [3–5], but similar microwave signals have also recently been observed when dc spin current is injected into a magnetic nanostructure containing a vortex [6–9], the most common magnetization configuration topologically different from the uniformly magnetized "macrospin." Remarkably, vortex oscillations can be more coherent [6] or lead to larger power output [9] than uniform mode oscillations, and do not require an external applied magnetic field [6, 9], thus reducing the complexity of potential applications.

While the electronic transport properties of spin-torque oscillators have been studied previously, the details of their magnetic structure and dynamics have remained hidden to experiments. In this Letter we present the first images of the ground-state vortex structure in a 3-dimensional (3D) nanopillar and of its steady-state oscillation induced by a dc spin current. In particular, we report real space, time-resolved x-ray images of the precessing vortex core that produces microwave emission. The elemental selectivity of the x-ray technique allows us to isolate the magnetization of the magnetic layer of interest, while the combined high temporal and spatial resolution of time-resolved x-ray microscopy allows the underlying magnetization dynamics to be observed in detail. We find that the static vortex profile differs considerably from the often-assumed 2D idealized structure. In addition, when the vortex is excited by a dc current the orbit radius is of order 10 nm, much smaller than when driven by ac magnetic fields or currents [11, 12], but in agreement with micromagnetic simulations [6, 10] for nanopillars. The precession direction is determined by the core polarity, as for resonantly-driven vortices.

We studied devices with a spin valve structure as shown in Fig. 1, with a 60 nm-thick magnetic layer composed of $Ni_{81}Fe_{19}$ and a thinner (5 nm) magnetic layer composed of $Co_{60}Fe_{20}B_{20}$, separated by a 40 nm-thick Cu spacer. The samples were patterned into nanopillars having elliptical cross-section with a major axis of ∼170 nm and a minor axis of ∼120 nm. The transport properties were very similar to devices characterized previously [6]. To allow x-ray transmission, the Si wafer was etched, leaving the pillars suspended on 200 nm-thick low-stress silicon nitride windows. Persistent gigahertz-frequency voltage oscillations are excited when a direct current is applied corresponding to electrons flowing from the thin magnetic layer to the thick magnetic layer. The data reported here were obtained at zero magnetic field and at room temperature, where the linewidths were ∼10 MHz. Our x-ray experiments were carried out at the Advanced Light Source (ALS), using the Scanning Transmission X-ray Microscope (STXM) on beamline 11.0.2 [13]. The spatial resolution of the STXM is about 30 nm and the temporal resolution of our experiment is about 70 ps. The samples were excited by a direct current of ∼3-8 mA.

Typically the synchronization of magnetization dynamics to x-ray pulses relies on the "pump-probe" approach: the "pump" consists of pulses of magnetic field or electric current to study the response to transient excitations or continuous sinusoidal signals to study resonant behaviors, while the "probe" consists of circularly polarized x-ray pulses. However, since in our experiment the dynamics are driven by a direct current instead of pulses or ac signals, achieving synchronization between the sample and the x-ray source requires a different technique. We developed a method that relies on injection locking [14] to phase lock the dc driven oscillation and a small ac current $i_{\rm sync}$. Fig. 1 shows the schematic of our setup: a direct current $I_{\rm DC}$ was applied to the sample to excite the steady-state GHz oscillation, a small alter-

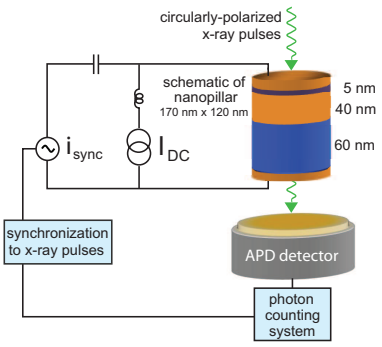

FIG. 1: (color online) Schematic of the experimental setup. The sample is positioned perpendicular to the incoming x-ray pulses and the transmitted x-ray intensity is recorded by an avalanche photodiode (APD) detector.

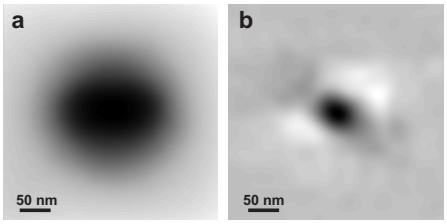

FIG. 2: Static STXM image and magnetic image. (a) STXM image showing mainly topographic contrast. (b) Magnetic image deduced from STXM images showing XMCD contrast corresponding to the out-of-plane magnetization.

nating current $i_{\rm sync}$ was added to $I_{\rm DC}$ to synchronize the sample oscillation to x-ray pulses. The synchronization procedure consists in first tuning the oscillator close to a frequency compatible with the x-ray pulse repetition rate by adjusting the current, then turning on i_{sync} with a frequency synchronized to the pulses. The root mean square value of the phase-locking current $i_{\rm sync}$ was less than 7% of the direct current which drives the magnetization dynamics. Electrical measurements of the linewidth and power emitted as a function of $i_{\rm sync}$, performed on a similar device, show that phase locking occurs already when $i_{\rm sync}$ is $\sim 0.03 I_{\rm DC}$ [19]. A photon counting system [15] was developed to distribute the x-ray transmission signals recorded by an avalanche photodiode detector (APD) to 16 different channels, corresponding to 16 equally-spaced phases of the oscillation.

To probe the thick magnetic layer, the x-ray energy was tuned to the Ni L_3 edge and STXM images of the sample transmission intensity $I^+(x,y)$ and $I^-(x,y)$ were recorded using right and left circularly polarized x-rays. Fig. 2(a) is a typical x-ray transmission image of our sample where topography contrast strongly dominates over magnetic contrast. The darker regions indicates the position of the nanopillar, which absorbs x-rays more strongly than the surrounding silicon nitride. To suppress the topography contrast, we computed the normalized difference $\frac{I^+(x,y)-I^-(x,y)}{I^+(x,y)+I^-(x,y)}$, and the resulting image of the differential intensity is shown in Fig. 2(b). The magnetic contrast of this figure comes from the X-ray Magnetic Circular Dichroism (XMCD) effect [16]. The sample surface is perpendicular to the x-ray propagation direction, thus the contrast in Fig. 2(b) corresponds to the out-of-plane magnetization of the thick layer.

We studied both the equilibrium magnetic state of these samples without any external excitation and the persistent oscillations excited by a direct current. The static measurement shown in Fig. 2(b) confirms that the magnetic configuration of the thick layer is a vortex. However, besides the black area in the center of the image corresponding to the vortex core, there are also two lighter regions indicating a considerable out-of-plane magnetization component with opposite orientation to that of the core. To depict this magnetization distribution more clearly, the pillar area in Fig. 2(b) is plotted in Fig. 3 (top) using both pseudocolor and a surface plot, where the height is proportional to the out-of-plane magnetization. The observed distortions indicate that the static vortex profile strongly deviates from an ideal vortex profile, where the magnetization would lie in plane everywhere except at the core. The data also clearly show that the magnetization breaks the symmetry of the elliptical shape of the sample and is rotated with respect to the device long axis. Thus, although most studies of vortices in micro- and nano-scale magnetic elements have focused on idealized two-dimensional structures, our data show that the magnetic vortex as a ground state in a spin-torque nanopillar is more complicated.

To understand the static structure of the vortex we performed micromagnetic simulations on an isolated Permalloy (Py) pillar with the same dimensions as the thick layer in our samples, using the LLG Micromagnetic Simulator [17] (bottom part of Fig. 3). We find that the out-of-plane component of the simulated magnetization on the top and bottom surfaces also breaks the in-plane symmetry, looking similar to the data. The variation of the magnetization distributions from the top surface to the bottom surface results from the fact that the 60 nm thickness of our vortex layer is comparable to the lateral size [18] and is also considerably larger than the exchange length for Permalloy, which is only about 5 nm. Although the XMCD contrast deduced from x-ray transmission images corresponds to the magnetization averaged along the entire normal axis of the vortex layer, the data are similar to the simulated magnetization distribution at the top or bottom surfaces of the Py pillar, but not to the simulation average over the whole thickness. In the simulations the two surfaces exhibit mirror symmetry, leading to a cancellation of the rotations when performing the average. We conclude that the rotation of the magnetization seen in the data is due to asymmetry in the experimental device, arising from interlayer coupling, the tapered

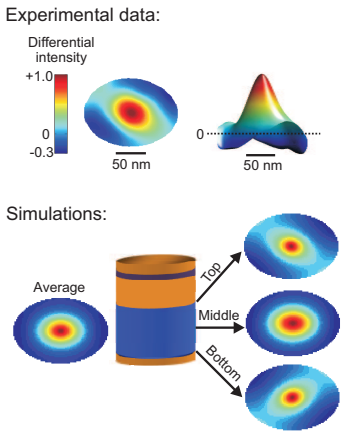

FIG. 3: (color online) Comparison of experimental data and micromagnetic simulation of the static magnetization distribution. Top: The magnetic contrast within the sample area of the magnetic image, Fig. 2(b), with pseudo color (left) and its surface plot (right), where the height is proportional to the out-of-plane magnetization. Bottom: Micromagnetic simulation, showing the out-of-plane component of the equilibrium magnetization in different planes of an isolated 60 nm-thick Py pillar with the same dimensions as in our sample (as shown).

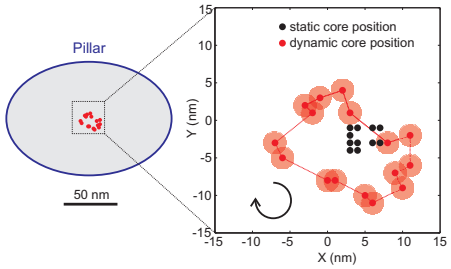

FIG. 4: (color online) Vortex core trajectory deduced from STXM images. Black dots: static core positions recorded by 16 photon counters. (Some of the static positions overlap.) Red dots: core positions of the same sample during the oscillations, recorded by the same photon counters. Red disks: an estimate of the position uncertainty by using the standard deviation of the static core positions. The direction of vortex gyration is clockwise, as indicated.

profile of the device sidewalls and possibly other shape non-idealities. In short, the non-ideal vortex profile revealed in our x-ray data can be understood as follows: first the 3D nature of the thicker layer allows the magnetization structure to rotate as a function of position along the thickness of the layer; second, the mirror symmetry between top and bottom surfaces is also broken due to the asymmetric environment.

Our measurements of the 16 evenly-spaced phases of the magnetization dynamics directly confirm that the GHz-frequency GMR signal observed under dc bias [6] originates from the vortex translational mode [19]. Fig. 4 shows the vortex core trajectory (red) of a sample oscillating at 0.95 GHz, excited by a direct current of 7.8 mA (i_{sync} ∼0.4 mA RMS). No dynamics are observed when i_{sync} is present but $I_{DC} = 0$. The core positions for the same sample without any excitation (black dots in Fig. 4) are recorded by the same photon counting system used for the dynamic measurement. Thus we can use the standard deviation of the recorded static core positions to estimate the uncertainty of the vortex core trajectory (transparent red disks in Fig. 4).

From the dynamics data taken on the same device as the static data we determine the radius of the vortex trajectory, which we find to be ∼10 nm. The radius is much smaller than that seen in resonating vortex core gyration excited in single-layer devices by ac magnetic field (∼100 nm in Ref. 11), ac current (∼250 nm in Ref. 12), or dc driven vortex gyration in a metallic nanocontact to an extended film with an out-of-plane external magnetic field (∼158 nm in the simulations in Ref. 8). However, the smaller radius found here is in rough agreement with the value of ∼ 20 nm obtained based on transport measurements and micromagnetic simulations in Refs. 6 and 10, on a system similar to ours, and is also consistent with the emitted RF power from the vortex oscillator, which is less than ∼ 1% of the maximum power that would correspond to a full 360° rotation of the magnetization. A smaller gyration radius than in Refs. 8, 11 and 12 might be expected due to the stronger geometrical confinement in our devices (∼100 nm lateral dimensions vs. 500 nm or more in the cited experiments) [20]. We note that since the simulations in Refs. 6 and 10 were performed without ac current this agreement suggests that the ac current values in the x-ray experiment have only a weak effect on the orbit.

Time-resolved images for the same sample, but having the opposite core polarity due to its magnetic history (as evidenced by the change from white to black contrast in the center of the normalized difference images) reveal that the core moves counterclockwise, opposite to the direction of gyration for the case shown in Fig. 4 [19]. Thus, we find that the vortex core rotation direction is uniquely determined by the internal structure of the vortex, just as for a freely relaxing magnetic vortex [21], even when the spin-torque, an intrinsically nonlinear effect, is strong enough to balance the damping.

Analytical models of vortex dynamics have assumed an "ideal" 2D vortex profile where the magnetization is uniform along the normal axis and the in-plane distribution maintains the sample topographic symmetry [22, 23]; however, our data, in conjunction with the simulations (Fig. 3), suggest that these models may not be strictly applicable to vortices in nanopillar spin valves due to the 3D nature of the magnetization distribution. Most strikingly, analytical models based on Thiele's equation [24, 25] and that assume an ideal vortex structure predict that uniform in-plane spin polarization should

not excite stable vortex gyration [8, 26]. Under these assumptions, only the perpendicular component of the spin polarization should sustain persistent vortex gyration, while the in-plane component should lead only to vortex core displacement. In contrast, our x-ray data clearly show that in our samples the vortex undergoes steady-state oscillation under the influence of a predominantly in-plane spin-polarized longitudinal current (the thin magnetic layer does not have detectable out-of-plane magnetization, non-uniform in-plane magnetization, or spin dynamics within our measurement sensitivity [19]). We suggest that a possible reason for the discrepancy is the unusual profile of the vortex in spin valve nanopillars such as studied here. Since both damping and spin-torque are strongly dependent on the vortex magnetization distribution, models that assume an idealized vortex configuration may not be accurate for the non-ideal vortex structure we observe in spin-torque nanopillars, but more work is needed for a full understanding. On the other hand, the analytical prediction that a uniform in-plane polarized spin current should not induce gyration at all in the ideal case suggests that spin-torque driving might be rendered more efficient by using nonuniform polarizers [26, 27].

In summary, we presented the first space- and time-resolved images of steady-state magnetization dynamics in a dc-driven spin-torque oscillator. We find that the vortex precession direction is determined by the core polarity, and that the orbit radius is on the order of 10 nm, in agreement with micromagnetic simulations. We also observe that the vortex profile in spin-valve nanopillars deviates from the often-assumed 2D structure. We suggest that this non-ideality, currently not taken into account by analytical models, plays an important role in the excitation of the oscillations.

The x-ray work was performed at the Advanced Light Source in Berkeley which, like the work of the SLAC/Stanford authors, is supported by the US Department of Energy, Office of Basic Energy Sciences. X. W. Y. acknowledges support from the ALS. The Cornell authors acknowledge support from the Office of Naval Research, the Army Research Office, and the NSF through its NSEC program. The research was performed in part at the Cornell NanoScale Facility, which is supported by the NSF.

* These authors contributed equally to this work; corresponding authors.

[1] J. C. Slonczewski, J. Magn. Magn. Mater. **159**, L1 (1996).
[2] L. Berger, Phys. Rev. B **54**, 9353 (1996).
[3] J. Katine and E. E. Fullerton, J. Magn. Magn. Mater. **320**, 1217 (2008).
[4] D. Berkov and J. Miltat, J. Magn. Magn. Mater. **320**, 1238 (2008).
[5] T. Silva and W. Rippard, J. Magn. Magn. Mater. **320**, 1260 (2008).
[6] V. S. Pribiag, I. N. Krivorotov, G. D. Fuchs, P. M. Braganca, O. Ozatay, J. C. Sankey, D. C. Ralph, and R. A. Buhrman, Nat. Phys. **3**, 498 (2007).
[7] M. R. Pufall, W. H. Rippard, M. L. Schneider, and S. E. Russek, Phys. Rev. B **75**, 140404(R) (2007).
[8] Q. Mistral, M. van Kampen, G. Hrkac, J.-V. Kim, T. Devolder, P. Crozat, C. Chappert, L. Lagae, and T. Schrefl, Phys. Rev. Lett. **100**, 257201 (2008).
[9] A. Ruotolo, V. Cros, B. Georges, A. Dussaux, J. Grollier, C. Deranlot, R. Guillemet, K. Bouzehouane, S. Fusil, and A. Fert, Nat. Nano. **4**, 528 (2009).
[10] G. Finocchio, V. S. Pribiag, L. Torres, R. A. Buhrman, B. Azzerboni, Appl. Phys. Lett. **96**, 102508 (2010).
[11] M. Curcic, B. V. Waeyenberge, A. Vansteenkiste, M. Weigand, V. Sackmann, H. Stoll, M. Fähnle, T. Tyliszczak, G. Woltersdorf, C. H. Back, et al., Phys. Rev. Lett. **101**, 197204 (2008).
[12] M. Bolte, G. Meier, B. Krüger, A. Drews, R. Eiselt, L. Bocklage, S. Bohlens, T. Tyliszczak, A. Vansteenkiste, B. V. Waeyenberge, et al., Phys. Rev. Lett. **100**, 176601 (2008).
[13] A. L. D. Kilcoyne, T. Tyliszczak, W. F. Steele, S. Fakra, P. Hitchcock, K. Franck, E. Anderson, B. Harteneck, E. G. Rightor, G. E. Mitchell, et al., J. Synchrotron Radiat. **10**, 125 (2003).
[14] W. H. Rippard, M. R. Pufall, S. Kaka, T. J. Silva, S. E. Russek, and J. A. Katine, Phys. Rev. Lett. **95**, 067203 (2005).
[15] J. P. Strachan, V. Chembrolu, X. W. Yu, T. Tyliszczak, and Y. Acremann, Rev. Sci. Instrum. **78**, 054703 (2007).
[16] G. Schütz, W. Wagner, W. Wilhelm, P. Kienle, R. Zeller, R. Frahm, and G. Materlik, Phys. Rev. Lett. **58**, 737 (1987).
[17] M.R. Scheinfein, LLG Micromagnetic Simulator^{TM}, http://llgmicro.home.mindspring.com.
[18] R. Hertel, O. Fruchart, S. Cherifi, P.-O. Jubert, S. Heun, A. Locatelli, and J. Kirschner, Phys. Rev. B **72**, 214409 (2005).
[19] See EPAPS document No.XXXX. For more information on EPAPS, see http://www.aip.org/pubservs/epaps.html.
[20] K. Y. Guslienko, G. R. Aranda, and J. M. Gonzales, arXiv:0912.5521v1.
[21] S.-B. Choe, Y. Acremann, A. Scholl, A. Bauer, A. Doran, J. Stöhr, and H. A. Padmore, Science **304**, 420 (2004).
[22] K. Y. Guslienko, X. F. Han, D. J. Keavney, R. Divan, and S. D. Bader, Phys. Rev. Lett. **96**, 067205 (2006).
[23] B. A. Ivanov and C. E. Zaspel, Appl. Phys. Lett. **81**, 1261 (2002).
[24] A. A. Thiele, Phys. Rev. Lett. **30**, 230 (1973).
[25] D. L. Huber, Phys. Rev. B **26**, 3758 (1982).
[26] A. V. Khvalkovskiy, J. Grollier, N. Locatelli, Ya. V. Gorbunov, K. A. Zvezdin, and V. Cros, Appl. Phys. Lett. **96**, 212507 (2010).
[27] V. S. Pribiag, G. Finocchio, B. J. Williams, D. C. Ralph, and R. A. Buhrman, Phys. Rev. B **80**, 180411(R) (2009).